Reaction Kinetics, Mechanisms and Catalysis (2020) 129:659–677
https://doi.org/10.1007/s11144-020-01749-0

Oxovanadium(IV) complex supported on the surface of magnetite as a recyclable nanocatalyst for the preparation of 2-amino-4*H*-benzo[*h*]chromenes and selective oxidation of sulfides

Niaz Monadi[1] · Hoda Davoodi[1] · Milad Aghajani[1]

Received: 11 December 2019 / Accepted: 13 February 2020 / Published online: 27 February 2020

Abstract

In this work, an oxovanadium(IV) complex supported on the surface of modified Fe_3O_4 with a silica shell has been synthesized. The obtained nanostructures were characterized using FT-IR, XRD, SEM, EDX, VSM, TGA and ICP-AES analyses. The synthesized magnetic nanocatalyst has been applied as an efficient catalyst for the synthesis of 2-amino-4*H*-benzo[*h*]chromenes via three-component one-pot reaction and also selective oxidation of sulfides to sulfoxides under solvent-free conditions. The synthesized nanocatalyst could be easily separated from the reaction mixture using an external magnet and reused several consecutive runs for both reactions without noticeable reducing in its catalytic activity.

Keywords Oxovanadium complex · Magnetic nanoparticles · Recyclable nanocatalyst · 2-amino-4*H*-chromene derivatives · Sulfoxidation

Introduction

Heterogeneous supported nanocatalysts are an important, versatile reagents and emerging field in catalysis science, because of the small size, the active metal atoms are exposed to the surface and thus minimize the specific cost per function [1–3]. Despite the high activity and selectivity of homogeneous catalysts, the use of heterogeneous catalytic systems has been favored over the use of homogeneous ones. The major disadvantage of metal-based homogeneous catalyst systems is their difficult

Electronic supplementary material The online version of this article (https://doi.org/10.1007/s11144-020-01749-0) contains supplementary material, which is available to authorized users.

✉ Niaz Monadi
Nimonadi@umz.ac.ir

[1] Department of Inorganic Chemistry, Faculty of Chemistry, University of Mazandaran, Babolsar 47416-95447, Iran

separation from the reaction solution by classical methods as well as they may possibly leave toxic traces of heavy metals in the products. Hence, such drawbacks can be overcome by immobilization of a catalytically active molecule on a solid support [4–13]. From the various solid supports, magnetic nanoparticles (MNPs) such as Fe_3O_4 are valuable supports for the immobilization of inorganic and organic catalysts due to their unique advantages including high dispersion, low toxicity, good degree of chemical stability and high active surface for adsorptions or immobilization of metals and ligands. On the other hand, MNPs can be separated by magnetic decantation after the reaction, which is easier rather than cross flow filtration and centrifugation, thus making it a more sustainable nanosupprt [14–18].

Although numerous developments have been achieved in the synthesis and application of magnetic nanoparticles but unfortunately, they sometimes tend to aggregate in a liquid phase due to the anisotropic dipolar attraction. Hence, it is crucial to develop efficient strategies to strengthen the chemical stability of magnetic nanoparticles. In order to resolve such problems, the magnetic cores are usually protected with an outer stabilizing or coating materials, such as organic (polymers and surfactants) and inorganic (silica and carbon-based materials) stabilizers [19–21]. These coating materials not only provide stability to the magnetic nanoparticles but they also generate a type of high-performance composite materials that can be used in a wide range of research protocols, such as Mannich type reactions, carbon–heteroatom bond formation, coupling reactions, alkylation, oxidation, reductions, asymmetric synthesis and biology related ones [22–28]. Hence, many efforts have been devoted to immobilize various metal complexes (e.g., Sc, Cu, Fe, Mn, Co, Ni, Mo and V) on magnetite with silica shell as heterogeneous nanocatalysts for various organic transformations [29–38].

The selective oxidation of sulfides as environmental pollutants to sulfoxides is an important transformation in organic chemistry. Moreover, a basic obstacle during the oxidation of sulfides is overoxidation of the sulfoxides to their corresponding sulfones. Therefore, it is very important that the catalyst has a high selectivity. Some of biologically active sulfoxides play an important role as therapeutic agents such as antifungal, antibacterial, anti-atherosclerotic, anti-ulcer, antihypertensive and anti-atherosclerotic as well as psychotropic and vasodilators [39, 40].

Multi-component reactions (MCRs) have recently gained prime interest in field of organic synthesis due to their ability of building up the complex molecules in a single step. Nowadays, MCRs are considered as a substantial route in the synthesis of many important heterocyclic compounds such as chromene derivatives. 2-Amino-4*H*-chromenes are an important class of natural oxygen-containing heterocyclic compounds, which are extensively found in edible fruits, vegetables and used in cosmetics and pigments. Derivatives of these compounds are known to possess antibacterial, antifungal, antioxidant, antitumor, important pharmaceutical and other bioorganic properties [41–43].

Owing to the context of green chemistry and heterogeneous nanocatalysis, we herein report an oxovanadium(IV) complex supported on modified Fe_3O_4 by a stepwise procure and study its catalytic performance for preparation of 2-amino-4*H*-benzo[*h*]chromene derivatives in an one-pot three-component reaction and also selective oxidation of sulfides under solvent-free condition.

Experimental section

Materials and measurements

All the chemicals and solvents without any further purification were analytical reagent grade where purchased from Aldrich, Merck or Fluka. FT-IR spectra of nanostructures were recorded using KBr disks on a Bruker vector 22 instrument in the spectral range 4000–400 cm^{-1}. Thermogravimetric (TGA) analysis was performed on a Perkin Elmer analyzer under nitrogen atmosphere from room temperature to 800 °C. Ultrasonic irradiation was carried out with a SONICA-2200 Ep, input 50–60 Hz/305 W. The nanoparticles were analyzed using a Holland Philips X Pert X-ray diffraction diffractometer with Cu Kα radiation (λ = 1.5404 Å) in the 2θ range of 10°–70° at room temperature. Scanning electron microscopy (SEM) images were recorded with a VEGA/TESCAN KYKY-EM3200 microscope. Magnetic properties of samples were detected at room temperature from − 10,000 to + 10,000 Oe using a vibrating sample magnetometer (VSM, Meghnatis Kavir Kashan Co., Kashan, Iran). The metal content of the catalysts was measured by inductively coupled plasma atomic emission analysis (ICP-AES, Varian company VISTA-PRO model).

Synthesis of oxovanadium complex supported on modified Fe_3O_4 nanoparticles (Fe_3O_4@SiO_2@VO) as nanocatalyst

Iron oxide magnetic nanoparticles (Fe_3O_4), silica-coated Fe_3O_4 nanoparticles (Fe_3O_4@SiO_2) and functionalized Fe_3O_4 nanoparticles with amine group (Fe_3O_4@SiO_2-amine) were synthesized according to the literature method [14, 44, 45]. For synthesis of the nanocatalyst, brown solid Fe_3O_4@SiO_2-amine (0.3 g) and $VO(acac)_2$ (5 mmol, 1.32 g) were sonicated in 30 mL dry toluene for 5 min. Then, the suspended mixture was refluxed for 24 h under N_2 atmosphere. The final product was isolated by magnetic decantation and washed with ethanol/dry toluene and then dried at 80 °C. In the next step, in order to remove the unreacted $VO(acac)_2$, Soxhlet extraction was carried out with ethanol.

General procedure for the synthesis of 2-amino-4*H*-benzo[*h*] chromenes

A mixture of aldehyde (1 mmol), 1-naphthol (1 mmol), malononitrile (1 mmol), and Fe_3O_4@SiO_2@VO(IV) (0.2 g) was heated to 125 °C under solvent-free conditions. Using TLC, the progress of the reaction was controlled until the aldehyde had disappeared. After completion of the reaction, the resulting mixture was cooled to room temperature and the nanocatalyst separated using an external magnet, washed with ethanol, dried and then reused in next run. The obtained products were filtered and

washed with ethanol to remove any unreacted starting materials. The synthesized 2-amino-4*H*-benzo[*h*]chromene derivatives were crystallized from hot ethanol in order to gain pure products.

General procedure for oxidation of sulfides

In a typical experiment, a mixture of sulfide (1.0 mmol), TBHP (2 mmol) and the nanocatalyst (50 mg) were added in a round-bottom flask and stirred under solvent-free condition in room temperature. Then, the mixture was stirred for the appropriate time at room temperature. The progress of the reaction was monitored by TLC. After completion of the reaction, the nanocatalyst was separated by magnetic decantation, washed with water/ethanol and reused for subsequent recycling runs. Also, the corresponding product was dried over anhydrous Na_2SO_4. All the experiments were carried out three times and mean value for each experiment was reported in this study for accuracy of the results.

Selected spectral data

All obtained products were characterized by FT-IR and melting point [46–48]. Also, ^{1}H and ^{13}C NMR spectra for some of 2-amino-4*H*-benzo[*h*]chromenes are reported (see the supporting information). Some of selected spectroscopic data is provided as below.

2-Amino-4-(4-chlorophenyl)-4*H*-benzo[*h*]chromene-3-carbonitrile: ν_{max} (KBr) 3468, 3327, 2192,1669, 1599, 1407,1374, 1101 cm^{-1}; δ_H (400 MHz, $CDCl_3$): 4.82 (br s, 2H, NH_2), 4.88 (s,1H, CH), 7.01–8.20 (10H, Ar).

2-Amino-4-(4-nitrophenyl)-4*H*-benzo[*h*]chromene-3-carbonitrile: ν_{max} (KBr) 3473, 3349, 2191,1650, 1624,1511,1402,1350, 1099 cm^{-1}; δ_H (400 MHz, $CDCl_3$): 4.90 (br s, 2H, NH_2), 5.0 (s,1H, CH), 6.96–8.22 (10H, Ar).

2-Amino-4-(3-nitrophenyl)-4H-benzo[h]chromene-3-carbonitrile: ν_{max} (KBr) 3470, 3328, 2192,1666, 1601,1525,1406,1375, 1102 cm^{-1}; δ_H (400 MHz, CD_3CN): 5.73 (br s, 2H, NH_2), 5.09 (s,1H, CH), 7.04–8.30 (10H, Ar).

Results and discussion

Preparation and characterization of the nanostructures

The procedure for the covalent attachment of oxovanadium(IV) complex immobilized on the surface of modified Fe_3O_4 nanoparticles is depicted in Scheme 1. In the first step, bare Fe_3O_4 nanoparticles were synthesized using Fe(III) and Fe(II) salts via a co-precipitation method. Subsequently, in order to protect the Fe_3O_4 nanoparticles from oxidation and agglomeration, silica shell was used. Then, modified Fe_3O_4 nanoparticles with a silica shell were functionalized with

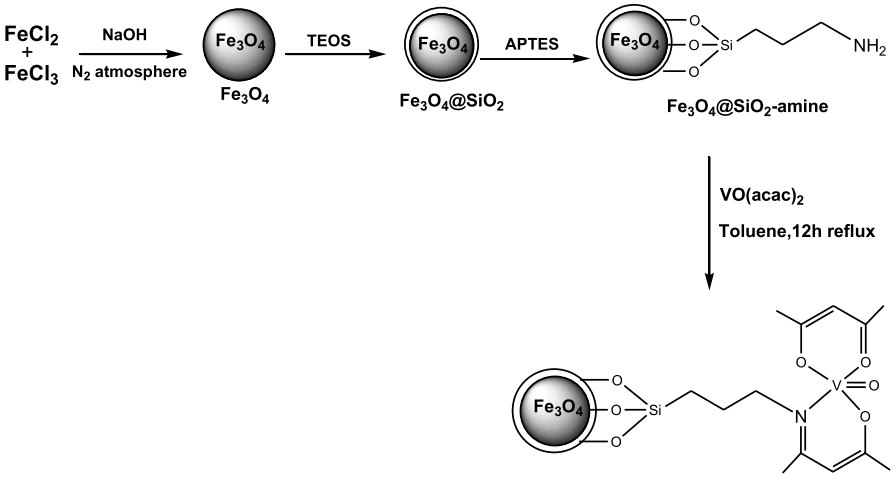

Scheme 1 Preparation process of Fe_3O_4@SiO_2@VO as nanocatalyst

3-aminopropyltriethoxysilane (APTES). Finally, $VO(acac)_2$ was reacted with functionalized Fe_3O_4 nanoparticles to obtain Fe_3O_4@SiO_2@VO as nanocatalyst.

The structural features of the prepared nanostructures were characterized by FT-IR, TGA, XRD, EDX, SEM, ICP-AES and VSM.

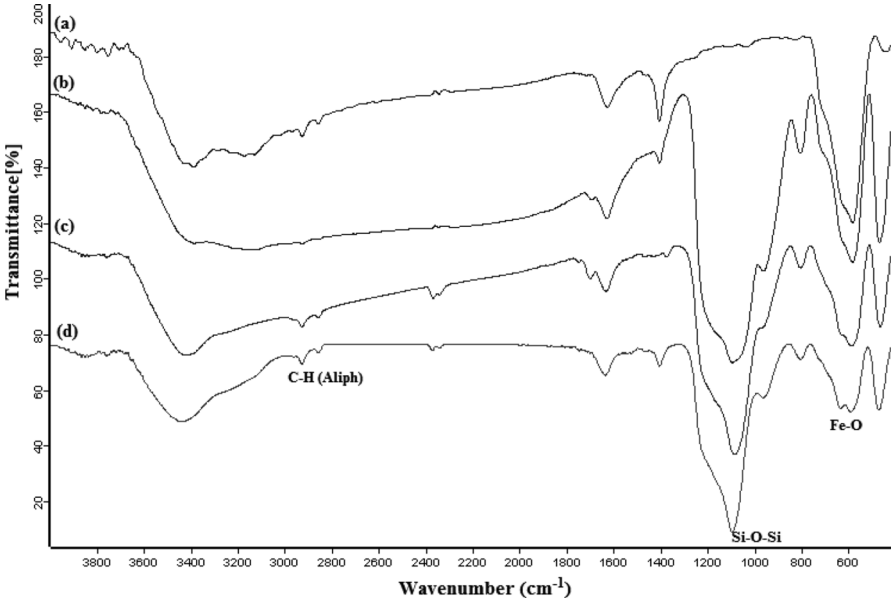

Fig. 1 FT-IR spectra for Fe_3O_4 (a), Fe_3O_4@SiO_2 (b), Fe_3O_4@SiO_2-amine (c) and Fe_3O_4@SiO_2@VO (d)

The FT-IR spectra of the nanostructures are shown in Fig. 1. In the FT-IR spectrum of the Fe_3O_4 (Fig. 1a), an intense broad band characteristic of the Fe–O at 578 cm^{-1} is observed. The broad band appearing around 3390 cm^{-1} is ascribed to O–H stretching of FeOH groups or adsorbed water of the magnetic surface. In the spectrum of Fe_3O_4@SiO_2 peaks at 577, 800 and 1089 cm^{-1} is assigned to the stretching mode of Fe–O, symmetric Si–O–Si and asymmetric Si–O–Si. These peaks have been indicated the formation of a silica layer on Fe_3O_4 nanoparticles (Fig. 1b). The FT-IR spectrum of Fe_3O_4@SiO_2-amine (Fig. 1c) shows a peak at 584 cm^{-1} assigned to Fe–O stretching vibration and bands at 799 and 1082 cm^{-1} are attributed to the symmetric and asymmetric of Si–O–Si, respectively. The presence of C–H vibration band at 2924 cm^{-1} confirmed the anchored APTES group on the surface of the silica. In the FT-IR spectrum of the Fe_3O_4@SiO_2@VO peaks at 581, 1093, 1630 and 2931 cm^{-1} are observed, which are due to Fe–O, Si–O–Si, C=N and $–CH_2$ group vibrations.

Fig. 2 shows the powder XRD patterns of Fe_3O_4, Fe_3O_4@SiO_2 and Fe_3O_4@SiO_2@VO. In the XRD pattern of Fe_3O_4 (Fig. 2a) observes six characteristic peaks at 2θ of 30.2°, 35.5°, 43.2°, 53.6°, 57.1°, and 62.7°, which is correspond to (220), (311), (400), (422), (511), and (440) reflections, respectively. These results were in agreement with standard data (JCPDS Card No. 19-629) and reveal that the Fe_3O_4 nanoparticles have inverse cubic spinel structured without impurity phases. The XRD pattern of Fe_3O_4@SiO_2 (Fig. 2b) reveals the same diffraction peaks to that of Fe_3O_4 nanoparticles. However, the observed broad peak about $2=\theta 20°–24°$ can be attributed to existence of amorphous silica. Compared with XRD pattern of Fe_3O_4 (Fig. 2a), almost no additional peaks are observed in XRD pattern of Fe_3O_4@SiO_2@VO (Fig. 2c) and just a slight decrease in the intensity of the diffraction peaks is observed. According to the obtained results, the

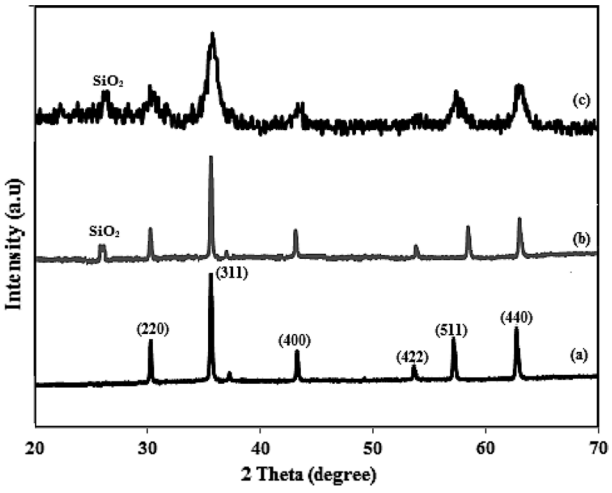

Fig. 2 XRD pattern for Fe_3O_4 (a), Fe_3O_4@SiO_2 (b) and the Fe_3O_4@SiO_2@VO (c)

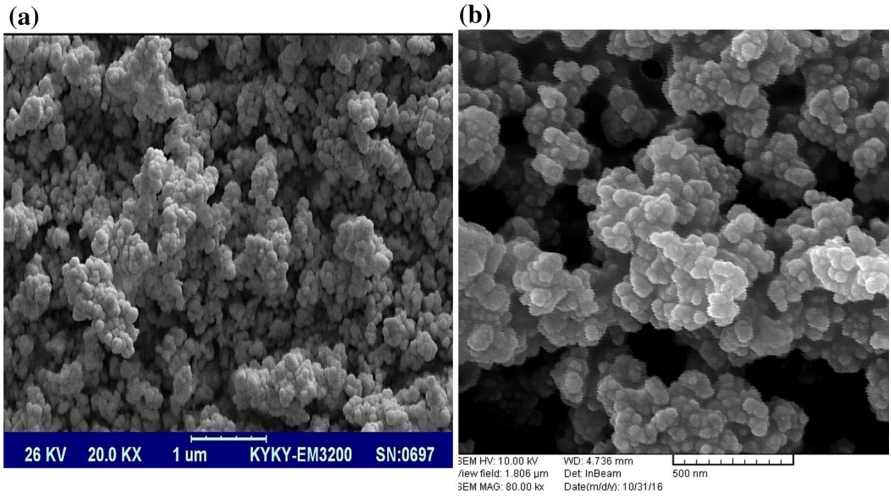

Fig. 3 SEM images of Fe_3O_4 (**a**) and Fe_3O_4@SiO_2@VO (**b**)

comparison of Fig. 2a–c shows that the characteristic peaks of Fe_3O_4 nanoparticles did not change after coating with silica and grafting of metal complex.

To investigate the morphology and sizes of the prepared nanostructure, SEM images were studied (Fig. 3). As it can be seen in Fig. 3a, Fe_3O_4 nanoparticles have approximately spherical morphology. The morphology of the nanocatalyst was also observed by FE-SEM, which contains a fairly uniform spherical shape

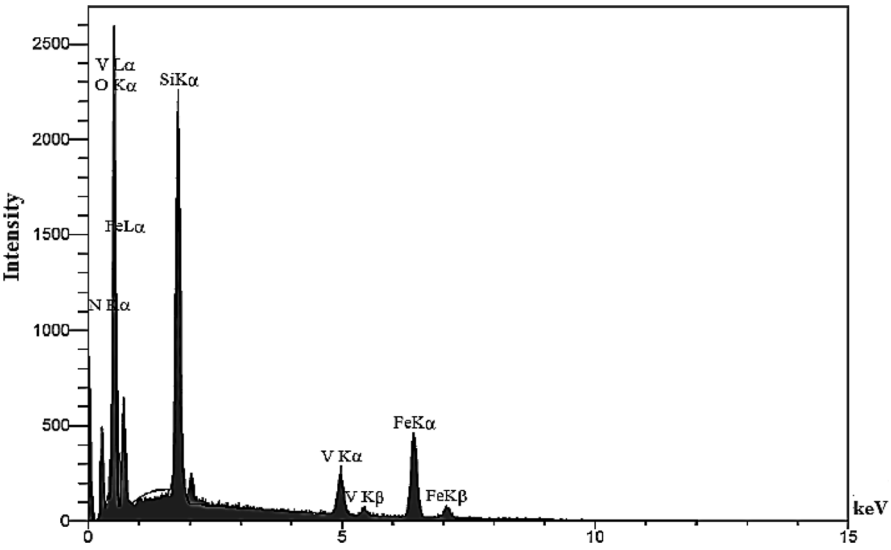

Fig. 4 EDX analysis of the Fe_3O_4@SiO_2@VO

and narrow size distributions (Fig. 3b). It is obvious that nanocatalyst still has the morphological features of the support except for a slightly larger particle size.

The EDX analysis of Fe_3O_4@SiO_2@VO indicate the presence of C, N, O, Si, Fe and V which provides further evidence for attachment of the vanadium complex on the surface of Fe_3O_4@SiO_2 (Fig. 4).

The magnetic properties of Fe_3O_4, Fe_3O_4@SiO_2 and Fe_3O_4@SiO_2@VO nanocatalyst were investigated by VSM at room temperature (Fig. 5). As can be observed, magnetization curves of the materials exhibited no remanence effect, which indicate superparamagnetic nature of the synthesized nanostructures. The specific saturation magnetization values for Fe_3O_4, Fe_3O_4@SiO_2 and Fe_3O_4@SiO_2@VO are 56.12, 38.59 and 30.04 emu g^{-1}. The decrease of magnetic saturation of the nanocatalyst indicates anchoring the metal complex on the surface of Fe_3O_4@SiO_2. Nevertheless, by using an external magnetic field and then removed it, the nanocatalyst can still be well re-dispersed, indicating that nanocatalyst possess good redispersibility and magnetic responsivity.

TGA analysis was carried out under N_2 atmosphere and the profiles are exhibited in Fig. 6. The profile of Fe_3O_4 shows a small weight loss (~3%) at about 100 ºC owing to the removal of physically adsorbed solvent and surface hydroxyl groups. As it can be seen, there is no significant weight loss in the range of 100–800 °C. Nonetheless, the profile of Fe_3O_4@SiO_2@VO shows two step weight losses. Initially shows a very similar weight loss in the range of 80–120 °C, which corresponds to removal of physically adsorbed solvents. Second mass loss happens above 210 °C (~21%), which is due to thermal decomposition of the organic chemicals (Fig. S1 in the Supplementary Information). Additionally, the loaded vanadium of the magnetic nanocatalyst was found to be 1.37 mmol g^{-1} based on ICP-AES analysis.

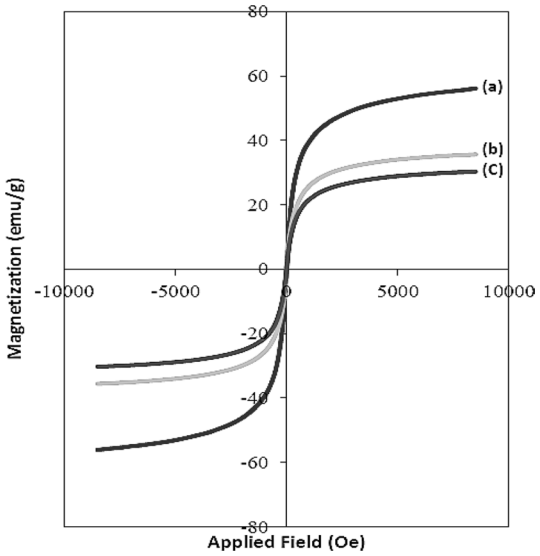

Fig. 5 Magnetization curves for Fe_3O_4 (a), Fe_3O_4@SiO_2 (b) and the Fe_3O_4@SiO_2@VO (c)

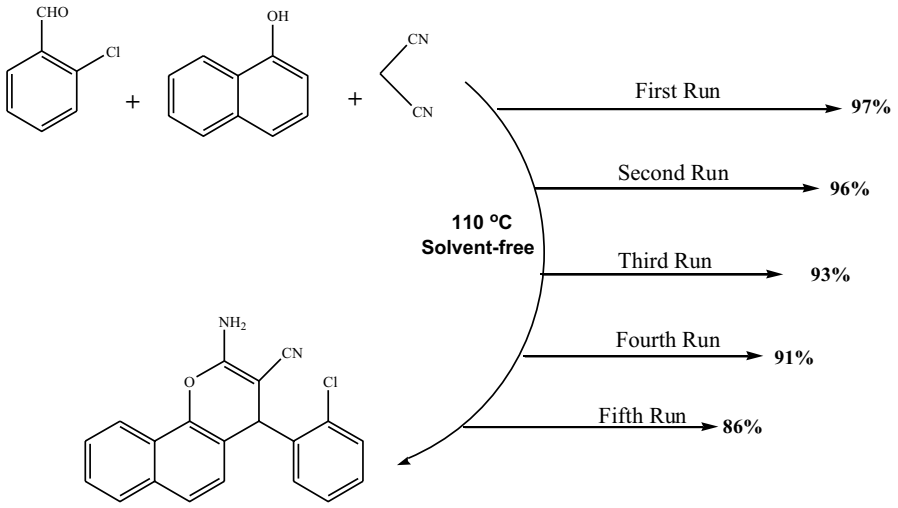

Fig. 6 Reusability test of the nanocatalyst for the model reaction (reaction condition: 0.2 g of the used nanocatalyst under solvent-free condition at 110 °C)

Catalytic performance of the synthesized nanocatalyst

Part A: Catalytic performance of Fe_3O_4@SiO_2@VO for the synthesis of 2-amino-4*H*-benzo[*h*]chromenes

After synthesis and characterization of Fe_3O_4@SiO_2@VO, we have been investigated its catalytic activity for the synthesis of 2-amino-4*H*-benzo[*h*]chromenes via the one-pot, three-component reaction of aldehydes, malononitrile and 1-naphthol. For this aim, the reaction of 2-chlorobenzaldehyde with malononitrile and 1-naphthol was chosen as a model reaction to obtain the optimization of the conditions. In order to investigate the effects of catalytic active centers, background reactions were performed (Table 1, entries 1–4). The use of Fe_3O_4, Fe_3O_4@SiO_2, and Fe_3O_4@SiO_2-amine instead of the nanocatalyst, the reaction did not proceed after 24 h. Also, this reaction was examined in the absence of the catalyst. It was found that when the reaction occurred without catalyst, it showed poor yield even after 24 h. Therefore, the existence of nanocatalyst is necessary for this reaction. To study optimum reaction conditions, the influences of various factors such as solvents, amount of the nanocatalyst and temperature, were studied. Initially, the effect of various solvents such as H_2O, EtOH, CH_3CN and also solvent-free condition were studied; highest catalytic activity was observed when solvent-free condition was employed (Table 1, entries 5–8). In the next step, amount of the nanocatalyst on catalytic activity was studied; which the best catalytic performance was obtained using 0.2 g of Fe_3O_4@SiO_2@VO. Increasing the amounts of the nanocatalyst obtain no further improvement (Table 1, entries 9–12). Also, The effect of temperature on the performance of the nanocatalyst was investigated. Among them, 110 °C was selected as the optimum temperature. At the above 110 °C, yield was decreased (Table 1, entries 13–16).

Table 1 Optimization and screening of the nanocatalyst for synthesis of desired product

Entry	Catalyst (amount)	Solvent	Temperature (°C)	Time	Yield[a]
1	Without catalyst	Solvent-free	110	24 h	trace
2	Fe_3O_4	Solvent-free	110	210 min	trace
3	Fe_3O_4@SiO_2	Solvent-free	110	120 min	trace
4	Fe_3O_4@SiO_2-NH_2	Solvent-free	110	60 min	trace
5	**Fe3O4@SiO2@VO (0.2 g)**	**Solvent-free**	**110**	**1 h**	**98%**
6	Fe3O4@SiO2@VO (0.2 g)	H2O	110	90 min	44%
7	Fe3O4@SiO2@VO (0.2 g)	EtOH	110	90 min	90%
8	Fe3O4@SiO2@VO (0.2 g)	CH_3CN	110	100 min	52%
9	Fe3O4@SiO2@VO (0.05 g)	Solvent-free	110	75 min	68%
10	Fe3O4@SiO2@VO (0.1 g)	Solvent-free	110	60 min	73%
11	Fe3O4@SiO2@VO (0.3 g)	Solvent-free	110	55 min	99%
12	Fe3O4@SiO2@VO (0.4 g)	Solvent-free	110	50 min	90%
13	Fe3O4@SiO2@VO (0.2 g)	Solvent-free	25	24 h	trace
14	Fe3O4@SiO2@VO (0.2 g)	Solvent-free	50	210 min	40%
15	Fe3O4@SiO2@VO (0.2 g)	Solvent-free	90	120 min	60%
16	Fe3O4@SiO2@VO (0.2 g)	Solvent-free	150	60 min	82%

All reactions were carried out with 2-chlorobenzaldehyde (1 mmol), malononitrile (1 mmol), and 1-naphthol (1 mmol)

Bold indicates the optimized conditions

[a]Isolated yield

Finally, after optimization of different parameters in three-component reaction of 2-chlorobenzaldehyde, malononitrile and 1-naphthol (0.2 g of the nanocatalyst under solvent free condition at 110 °C), we used the optimized reaction conditions to different aldehydes. As can be seen from Table 2, the electronic impacts indicate a minor effect on the reaction yield and this method tolerates various electron-poor and electron-rich aldehydes. The corresponding products obtain in good to excellent yields. However, the presences of electron-withdrawing substituents on the benzene ring were obtained the best results.

Nanocatalyst recycling and leaching test The reusability and stability of the anchored catalysts are a very important issue from practical, environmental and sustainability viewpoints [49]. The recyclability of the catalyst was surveyed using the reaction of 2-chloro benzaldehyde, malononitrile and 1-naphthol under the optimized conditions. In order to regenerate the nanocatalyst, after each run, it was separated by an external magnet, then washed several times with deionized water/EtOH and finally dried under vacuum for reuse. Fe_3O_4@SiO_2@VO could be recycled for at least five times without significant change in its activity (Fig. 6).

Study of metal leaching by ICP technique after the reusability test is an important issue. After the nanocatalyst was separated, the filtrate was used for ICP analysis as

Table 2 Synthesis of various 2-amino-4*H*-benzo[*h*]chromene derivatives using the Fe_3O_4@SiO_2@VO

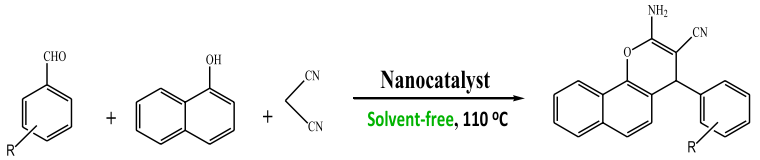

Entry	Aldehyde	Time (min)	Yield (%)[a]	Melting point (Observed) (°C)	Melting point (literature) (°C)[b]
1	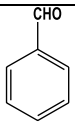	80	87	217–218	217–219
2	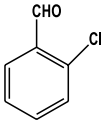	60	98	162–164	162–162
3	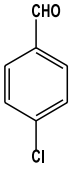	55	90	232–234	232–233
4		50	97	238–240	238–240
5	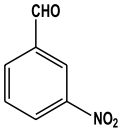	50	96	210–212	212–213
6	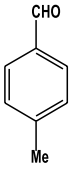	90	88	203–205	204–206
7	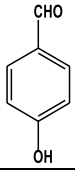	45	91	247–249	246–248

Table 2 (continued)

All reactions were carried out with aldehyde (1 mmol), malononitrile (1 mmol), and 1-naphthol (1 mmol) in the presence Fe3O4@SiO2@VO (0.2 g)under solvent-free condition at 110 ºC

[a]Isolated yield

[b]From Ref [46, 47]

leaching test. The vanadium leaching in the first and 5th run were 0.0012 (~ 0.14%) and 0.0029 mmol g^{-1} (~ 0.34%), respectively. Leaching experiments confirmed that the nanocatalyst is truly heterogeneous and that no catalytically active oxovanadium species are dissolved in the solution. It seems that strong interactions between the oxovanadium complex and magnetic support play a significant role in preventing metal leaching during the reaction.

SEM and FT-IR of the reused nanocatalyst after the 5th run in order to check the stability were studied. Based on SEM image, the morphology and structure of the reused nanocatalyst has been maintained during the recycling reaction (Fig. S2 in the Supplementary Information). Furthermore, FT-IR spectrum of the reused nanocatalyst was similar to that of fresh one and showed expected C–H, C=N, Si–O–Si and Fe–O vibration bands (Fig. S3 in the Supplementary Information). These results confirm the good stability and strong attachment of the oxovanadium complex on the surface of magnetic nanoparticles.

Proposed catalytic mechanism On the basis of some related literatures [50, 51], a plausible mechanism was proposed for the preparation of 2-amino-4*H*-benzo[*h*] chromenes using Fe_3O_4@SiO_2@VO (Scheme 2). According to the mechanism, the nanocatalyst could be attached to the carbonyl groups of the aldehyde and cyano group and activates it for nucleophilic attack. First, the reaction between malonitrile and aldehyde give an *α,β*-unsaturated nitrile (**I**) which reacts with 1-naphthol to form the dicyano compound (**II**). The rapid nucleophilic addition of phenolic hydroxyl group to the C=N group, and intramolecular cyclization to gives intermediate (III), after tautomerization of intermediate (III) forms the 2-amino-4*H*- benzo[*h*] chromenes (IV).

Part B: Catalytic performance of the nanocatalyst in the oxidation of sulfides

In continuation of our research in the area of developing homogeneous metal complexes supported onto surface of the magnetic support and their applications as catalyst in organic transformations [52–55], we were interested in finding a simple and efficient procedure for the selective oxidation of sulfides using synthesized nanocatalyst. The oxidation of sulfides was investigated in detail by optimizing the reaction variables such as solvent, substrate/oxidant molar ratio and amount of nanocatalyst. For this purpose, methyl phenyl sulfide was used as a sample.

At the first stage for optimization, the model reaction was carried out in the absence of nanocatalyst or oxidant (blank run). The result showed that reaction was incomplete even after prolonging the reaction time, which confirms the importance of the nanocatalyst and oxidant for the reaction completion (Table 3,

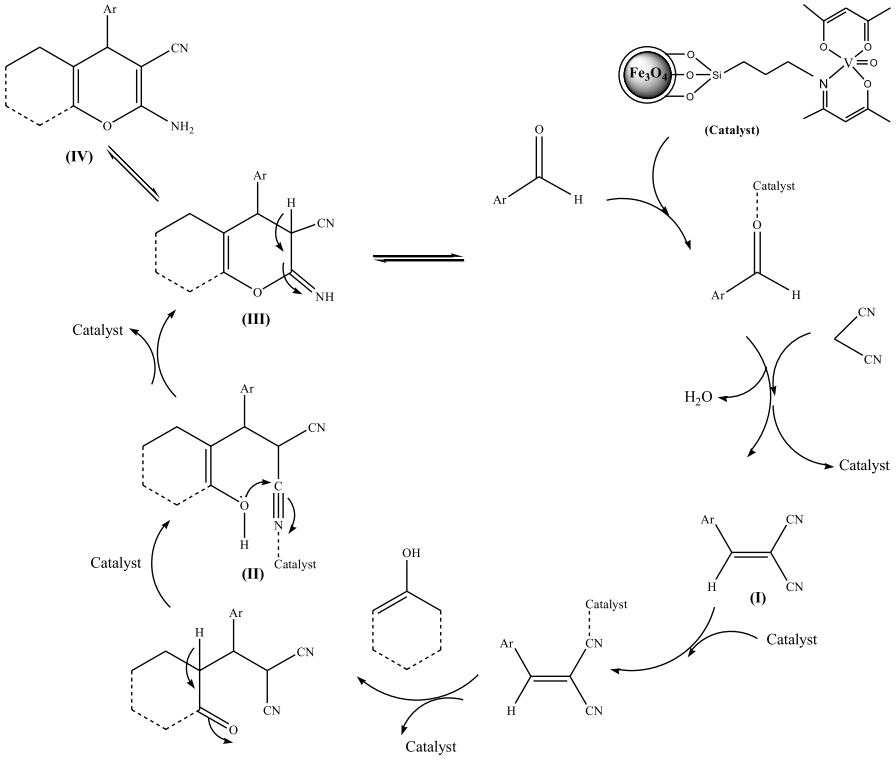

Scheme 2 Proposed mechanism for the preparation of 2-amino-4*H*-benzo[*h*]chromenes

entries 1–2). In continue the reaction was done in different solvents and also in solvent -free conditions (Table 3, entries 3–7 and 10). The results show that the highest conversion and selectivity is obtained under solvent-free condition within 2 h. However, it is noteworthy that the nanocatalyst is capable to act selectively in different solvents, which is a noticeable advantage. To optimize the amounts of nanocatalyst, different amounts of Fe_3O_4@SiO_2@VO (10, 30, 50 and 100 mg) were used in the oxidation of methyl phenyl sulfide using *tert*-butyl hydrogenperoxide (TBHP) under solvent-free condition (Table 2, entries 8–11). As observed, when 10 and 50 mg of catalyst were used, conversion was increased from 59 to 99% under same reaction conditions respectively. A further increase in the catalyst amount decreases the selectivity which is undesired. The effect of TBHP/substrate mole ratio on model reaction was investigated at regular intervals of time (Table 3, entries 10, 12 and 13). The maximum conversion and selectivity was observed at 2:1 mol ratio of TBHP/methyl phenyl sulfide. It should be noted that the use of Fe_3O_4, Fe_3O_4@SiO_2 and Fe_3O_4@SiO_2-amine instead of Fe_3O_4@SiO_2@VO gives a trace yield of the corresponding product even after 12 h (Table 3, entries 14–16).

Table 3 Optimization of reaction conditions in the oxidation of methyl phenyl sulfide as model substrate

Entry	Catalyst (amount)	Sulfide/TBHP ratio	Solvent	Time	Yield (selectivity to sulfoxide)[a]
1	–	1:2	Solvent-free	24 h	Trace
2	Fe3O4@SiO2@VO (50 mg)	without TBHP	Solvent-free	24 h	Trace
3	Fe3O4@SiO2@VO (50 mg)	1:2	MeOH	3 h	46%(100)
4	Fe3O4@SiO2@VO (50 mg)	1:2	EtOH	3 h	39%(100)
5	Fe3O4@SiO2@VO (50 mg)	1:2	H_2O	3 h	59%(100)
6	Fe3O4@SiO2@VO (50 mg)	1:2	CH_2Cl_2	3 h	33%(100)
7	Fe3O4@SiO2@VO (50 mg)	1:2	Toluene	3 h	21%(100)
8	Fe3O4@SiO2@VO (10 mg)	1:2	Solvent-free	4 h	59%(100)
9	Fe3O4@SiO2@VO (30 mg)	1:2	Solvent-free	3 h	71%(100)
10	Fe3O4@SiO2@VO (50 mg)	1:2	Solvent-free	2 h	> 99%(100)
11	Fe3O4@SiO2@VO (100 mg)	1:2	Solvent-free	1:30 h	> 99%(75)
12	Fe3O4@SiO2@VO (50 mg)	1:1	Solvent-free	3:30 h	> 99%(100)
13	Fe3O4@SiO2@VO (50 mg)	1:5	Solvent-free	1:45 h	> 99%(80)
14	Fe3O4 (50 mg)	1:2	Solvent-free	12 h	Trace
15	Fe3O4@SiO2 (50 mg)	1:2	Solvent-free	12 h	Trace
16	Fe3O4@SiO2-amine (50 mg)	1:2	Solvent-free	12 h	Trace

[a]Isolated yield

According to the experimental results (as it was shown in Table 3), solvent-free condition at room temperature using 50 mg of nanocatalyst and 2:1 mol ratio of TBHP to methyl phenyl sulfide during 2 h is the best choice for the model reaction (Table 3, entry 10). After optimization of different parameters for methyl phenyl sulfide reaction as model substrate, the catalytic activity of Fe_3O_4@SiO_2@VO was examined in the oxidation of other sulfides under the optimized conditions. The results have been summed up in Table 4. As it is clear, in all of the reactions, different sulfides were oxidized selectively to their corresponding sulfoxides in excellent yield in the short reaction times and no any by-products were observed. However, the lower activity of diaryl sulfide than arylalkyl

Table 4 Oxidation of sulfides in the presence of Fe_3O_4@SiO_2@VO using TBHP under solvent-free

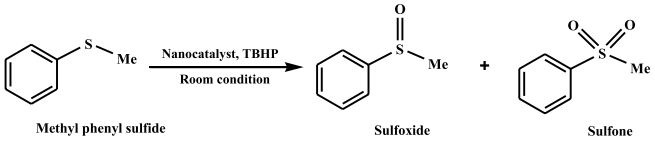

Methyl phenyl sulfide — Sulfoxide — Sulfone

Entry	Sulfide	Time (h)	Yield (%)[a]	Selectivity to sulfoxides (%)[a]	Observed melting point (literature)[b]
1	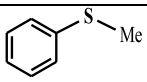	2	> 99	100	30–33 °C (33–34 °C)
2	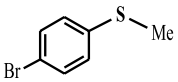	1:30	> 99	100	74–77 °C (74–76 °C)
3	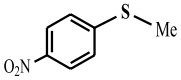	3	96	100	138–141 °C (140–141 °C)
4	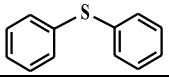	7	88	100	70–73 °C (69–71 °C)

Reaction condition: sulfide (1 mmol), TBHP (2 mmol), nanocatalyst (50 mg) and reaction was performed under solvent-free condition at room temperature

[a]Isolated yield on the basis of the weight of the pure product obtained

[b]From Ref. [48]

sulfides seems to be due to the steric hindrance of the diaryl group. Therefore, the obtained results show that this methodology will be applicable for the oxidation of a wide range of other sulfides.

Reusability and leaching test in the reaction of sulfides As the recyclability of a heterogeneous nanocatalyst is a significant factor, we investigated the recyclability and reusability of Fe_3O_4@SiO_2@VO was investigated under the optimized conditions. After the magnetic separation of nanocatalyst from the reaction mixture, the nanocatalyst was washed with ethanol/H_2O and dried to remove any remaining solvent, and then reused in the further reactions for several times. Results indicated that nanocatalyst is recyclable during six consecutive runs with preserving catalytic activity (Fig. 7).

Similar to previous section, a leaching test for methyl phenyl reaction under the optimized conditions was carried out. Only a low amount of vanadium leaching is observed (only 0.61% after 6th reaction run). Negligible amount of leaching during oxidation process confirms a strong interaction between magnetic support and metal complex and heterogeneous character of the synthesized nanocatalyst.

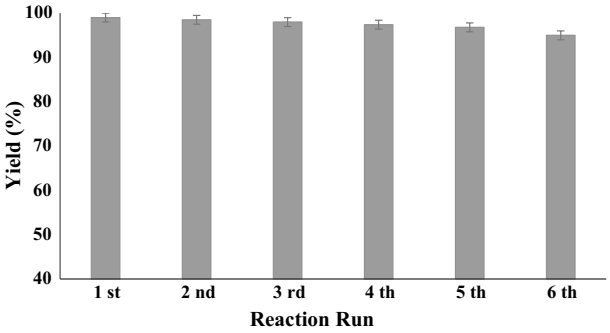

Fig. 7 Reusability test of the nanocatalyst in the oxidation of methyl phenyl sulfide as model substrate (reaction conditions: 50 mg of the used nanocatalyst with 2:1 mol ratio of TBHP to methyl phenyl sulfide under solvent-free condition at room temperature)

Table 5 Comparison catalytic activity of Fe_3O_4@SiO_2@VO with other reported catalysts in the reaction of 2-chlorobenzaldehyde, malononitrile and 1-naphtol (entries 1–4) and oxidation of methyl phenyl sulfide (entries 6–10)

Entry	Catalyst (amount)	Time	Solvent	Temp	Yield (selectivity)	References
1	Silica tungstic acid (0.1 g)	180 min	Solvent-free	120 ºC	90%	[56]
2	HTMAB (10 mol%)	240 min	H_2O	100 ºC	93%	[57]
3	$H_{14}[NaP_5W_{30}O_{110}]$ (0.03 g)	180 in	H_2O	100 ºC	91%	[58]
4	Fe_3O_4@SiO_2@Mo–Schiff base (0.2 g)	60 min	Solvent-free	125 °C	95%	[59]
5	Fe_3O_4@SiO_2@VO (0.2 g)	60 min	Solvent-free	110 ºC	98%	This work
6	Fe_3O_4/salen of Cu(II) (0.05 g)	180 min	EtOH	60 ºC	83% (-)	[60]
7	Ni(II)-salen-MCM-41 (0.02 g)	156 min	EtOH	Room condition	95% (-)	[61]
8	Polymer-anchored Cu(II) (0.05 g)	180 min	CH_3CN	Room condition	93% (90)	[62]
9	Cd(II)-salen-MCM-41 (0.02 g)	150 min	EtOH	Room condition	98% (-)	[61]
10	Cu/isatin@Fe_3O_4 (0.03 g)	360 min	EtOH	60 ºC	99% (97)	[63]
11	Fe_3O_4@SiO_2@VO (0.05 g)	120 min	Solvent-free	Room condition	> 99%(100)	This work

Comparison of catalytic efficiency with the previous works

In order to further investigate the eligibility of the present work, we compared this procedure with the previously reported catalysts for both reaction of 2-chlorobenzaldehyde, malononitrile and 1-naphtol for the preparation of corresponding product and oxidation of methyl phenyl sulfide, as shown in Table 5 [56–63] As can be seen, our catalytic system operated under mild conditions such as room temperature with minimum amounts of used catalyst in the oxidation of sulfides. Additionally, good stability of nanocatalyst, high product purity, commercially available materials and easy separation of the nanocatalyst are other advantages of this protocol.

Conclusions

In summary, we have reported a green, efficient and environmentally method for the synthesis of 2-amino-4*H*-benzo[*h*] chromene derivatives and selective oxidation of sulfide in the presence of oxovanadium(IV) complex immobilized on the surface of modified Fe_3O_4 nanoparticles as a nanocatalyst. The structure, morphology and chemical composition of the prepared nanostructures and nanocatalyst were confirmed by different spectroscopic and microscopic techniques like FT-IR, XRD, SEM, EDX, VSM, TGA, and ICP-AES analyses. Mild reaction conditions, use the green and non-toxic materials, good to excellent product yields, good stability of the nanocatalyst, ease of separation and recyclability of the catalyst and also use of solvent-free reaction conditions are the advantageous features of the presented work. It is noteworthy that the nanocatalyst also acted selectively in the oxidation of sulfide. Furthermore, the leaching experiments in the reaction of chromenes and sulfides proved that the oxovanadium complex was anchored firmly to the magnetic support. In addition, the results demonstrate that the nanocatalyst could be reused for several times in both reactions without significant loss in its activity.

Acknowledgements Authors gratefully acknowledge the University of Mazandaran Research Councils for financial support of this research project.

References

1. Bell AT (2003) Sciencece 299:1688–1691
2. Astruc D (2008) Nanoparticles and catalysis. Wiley, Weinheim, pp 1–48
3. Lu F, Astruc D (2020) Coord Chem Rev 408:213180
4. de Jong K (2009) Synthesis of solid catalysts. Wiley, Weinheim
5. Gupta K, Sutar AK, Lin C-C (2009) Coord Chem Rev 253:1926–1946
6. Aghajani M, Safaei E, Karimi B (2017) Synth Met 233:63–73
7. Saberikia I, Safaei E, Karimi B et al (2017) Chem Sel 2:11164–11171
8. Latypova AR, Tarasyuk IA, Filippov DV et al (2019) Reac Kinet Mech Cat 127:741–755
9. Kaluža L, Karban J, Gulková D (2019) Reac Kinet Mech Cat 127:887–902
10. Glotov A, Stavitskaya A, Chudakov Y et al (2019) Bull Chem Soc Jpn 92:61–69
11. Imaoka T, Yamamoto K (2019) Bull Chem Soc Jpn 92:941–948
12. Lin B, Lin Z, Chen S et al (2019) Dalton Trans 48:8279–8287

13. Kwak K, Lee D (2018) Acc Chem Res 52:12–22
14. Teja AS, Koh P-Y (2009) Prog Cryst Growth Charact Mater 55:22–45
15. Wang D, Astruc D (2014) Chem Rev 114:6949–6985
16. Rossi LM, Costa NJ, Silva FP, Wojcieszak R (2014) Green Chem 16:2906–2933
17. Schneider MGM, Lassalle VL (2017) Biomed Pharmacother 93:1098–1115
18. Bilal M, Zhao Y, Rasheed T et al (2018) Int J Biol Macromol 120:2530–2544
19. Tsang SC, Yu CH, Gao X, Tam K (2006) J Phys Chem B 110:16914–16922
20. Lien Y-H, Wu T-M (2008) J Colloid Interface Sci 326:517–521
21. Lu Y, Yin Y, Mayers BT, Xia Y (2002) Nano Lett 2:183–186
22. Reddy LH, Arias JL, Nicolas J, Couvreur P (2012) Chem Rev 112:5818–5878
23. Karimi B, Mansouri F, Mirzaei HM (2015) ChemCatChem 7:1736–1789
24. Lim CW, Lee IS (2010) Nano Today 5:412–434
25. Ghorbani-Choghamarani A, Darvishnejad Z, Norouzi M (2015) Appl Organomet Chem 29:170–175
26. Gawande MB, Branco PS, Varma RS (2013) Chem Soc Rev 42:3371–3393
27. Baig RN, Nadagouda MN, Varma RS (2015) Coord Chem Rev 287:137–156
28. Keshavarz M, Abdoli-Senejani M, Hojati SF et al (2018) Reac Kinet Mech Cat 124:757–766
29. Tamoradi T, Irandoust A, Ghadermazi M (2019) J Iran Chem Soc 16:1723–1733
30. Li Z, Wu S, Zheng D et al (2014) ChemPlusChem 79:716–724
31. Martins NM, Pombeiro AJ, Martins LM (2019) Catal Commun 125:15–20
32. Karimpour T, Safaei E, Karimi B, Lee YI (2018) ChemCatChem 10:1889–1899
33. Bezaatpoura A, Askarizadehb E, Akbarpoura SH, Amiria M, Babaei B (2017) Mol Catal 436:199–209
34. Zhou Q, Wan Z, Yuan X et al (2016) Appl Organomet Chem 30:215–220
35. Bhat PB, Rajarao R, Sahajwalla V et al (2015) J Mol Catal A 409:42–49
36. Bagherzadeh M, Bahjati M, Mortazavi-Manesh A (2019) J Organomet Chem 897:200–206
37. Veisi H, Rashtiani A, Rostami A et al (2019) Polyhedron 157:358–366
38. Khaledian D, Rostami A, Rouhani S (2019) Catal Commun 124:46–50
39. Fernández I, Khiar N (2003) Chem Rev 103:3651–3706
40. Kazemi M, Ghobadi M (2017) Nanotechnol Rev 6:549–571
41. Weber L (2002) Drug Discov Today 7:143–147
42. Chen M-N, Mo L-P, Cui Z-S et al (2019) Curr Opin Green Sustain Chem 15:27–37
43. Kohzadian A, Zare A (2019) Res Chem Intermed 45:5473–5485
44. Wang Z, Shen B, Aihua Z, He N (2005) Chem Eng J 113:27–34
45. Masteri-Farahani M, Tayyebi N (2011) J Mol Catal A 348:83–87
46. Kumar D, Reddy VB, Mishra BG, Rana R, Nadagouda MN, Varma RS (2007) Tetrahedron 63:3093–3097
47. Khurana JM, Nand B, Saluja P (2010) Tetrahedron 66:5637–5641
48. Weast RC, Astle MJ, Beyer WH (1989) CRC handbook of chemistry and physics, vol 1990. CRC Press, Boca Raton
49. Polshettiwar V, Luque R, Fihri A, Zhu H, Bouhrara M, Basset J-M (2011) Chem Rev 111:3036–3075
50. Ren Y-M, Cai C (2008) Catal Commun 9:1017–1020
51. Khoobi M, Ma'mani L, Rezazadeh F, Zareie Z, Foroumadi A, Ramazani A, Shafiee A (2012) J Mol Catal A 359:74–80
52. Aghajani M, Monadi N (2017) J Iran Chem Soc 14:963–975
53. Monadi N, Moradi E (2018) Transit Met Chem 43:161–170
54. Aghajani M, Monadi N (2018) Appl Organomet Chem. https://doi.org/10.1002/aoc.4433
55. Aghajani M, Monadi N (2019) J Chin Chem Soc 66:775–784
56. Farahi M, Karami B, Alipour S, Moghadam LT (2014) Acta Chim Slov 61:94–99
57. Jin TS, Zhang JS, Liu LB, Wang AQ, Li TS (2006) Synth Commun 36:2009–2015
58. Heravi MM, Bakhtiari Kh, Zadsirjan V, Bamoharram FF, Heravi MO (2007) Bioorg Med Chem Lett 17:4262–4265
59. Divsalar N, Monadi N, Tajbaksh M (2016) J Nanostruct 6:312–321
60. Ghorbani-Choghamarani A, Ghasemi B, Safari Z, Azadi G (2015) Catal Commun 60:70–75
61. Nikoorazm M, Ghorbani-Choghamarani A, Mahdavi H, Esmaeili SM (2015) Microporous Mesoporous Mater 211:174–181
62. Islam SM, Roy AS, Mondal P, Tuhina K, Mobarak M, Mondal J (2012) Tetrahedron Lett 53:127–131
63. Hajjami M, Kolivand S (2016) Appl Organomet Chem 30:282–288